









## Research Article

# Tribological Behavior on Stir-Casted Metal Matrix Composites of Al8011 and Nano Boron Carbide Particles

**N. Vinayaka,<sup>1</sup> K. G. Jaya Christiyan ,<sup>2</sup> Sarange Shreepad ,<sup>3</sup> S. N. Padhi ,<sup>4</sup>  
Sunil G. Dambhare ,<sup>5</sup> Ranjit kumar Puse ,<sup>6</sup> K. Gayathri ,<sup>7</sup>  
Aniket Bhanudas Kolekar ,<sup>5</sup> and S. Nagarajan ,<sup>8</sup>**

<sup>1</sup>Department of Aeronautical Engineering, Nitte Meenakshi Institute of Technology, Yelahanka, Bengaluru 560064, India

<sup>2</sup>Department of Mechanical Engineering, M S Ramaiah Institute of Technology, Bengaluru 560022, India

<sup>3</sup>Department of Mechanical Engineering, Ajeenkya D Y Patil School of Engineering, Lohegaon, Pune, India

<sup>4</sup>Department of Mechanical Engineering, Koneru Lakshmaiah Education Foundation, Vaddeswaram, Andhra Pradesh, India

<sup>5</sup>Department of Mechanical Engineering, Dr D Y Patil Institute of Engineering Management and Research, Akurdi, Pune 411044, India

<sup>6</sup>Department of Physical Science Chemistry, Rabindranath Tagore University, Bhopal, Madhya Pradesh, India

<sup>7</sup>Department of Physics, Academy of Maritime Education and Training, Kanathur, Chennai 603112, India

<sup>8</sup>Department of Mechanical Engineering, College of Engineering and Technology, Mettu University, Mettu, Ethiopia

Correspondence should be addressed to S. Nagarajan; [s.nagarajan@meu.edu.et](mailto:s.nagarajan@meu.edu.et)

Received 5 October 2022; Revised 29 October 2022; Accepted 24 November 2022; Published 15 February 2023

Academic Editor: Ramesh Balasubramanian

Copyright © 2023 N. Vinayaka et al. This is an open access article distributed under the Creative Commons Attribution License, which permits unrestricted use, distribution, and reproduction in any medium, provided the original work is properly cited.

The aluminum metal matrix composites were broadly exploited in the applications of automotive, aerospace, and other defense with functionally graded materials-related application. Above applications definitely required excellent mechanical characteristics. Therefore, in this way, the major attempt was made on the nano-based composites with aluminum alloy utilization. In this research, aluminum alloy AA8011 and the ceramic-based reinforcement particles of nano boron carbide ( $B_4C$ ) were selected for producing the metal matrix composites by the liquefying process or stir casting route. The weight percentage of nano boron carbide particles having 15 wt% was subjected to add into the aluminum alloy during the stir casting process. Then, processed nano boron carbide and AA8011 specimens were prepared to conduct tribological behaviors with various processing conditions like sliding velocity, setting wear temperature, and applied load by the tribometer setup. The scanning electron microscope was employed to examine the processed composites samples and worn-out surface samples. Finally, the multiobjective optimization was used to measure the individual performances of the tribological parameters by the gray relational technique.

## 1. Introduction

Aluminum-based metal matrix composites are well-admired materials to produce the enhanced composites material by the addition of exclusive strength and maximum modulus of elasticity. Owing to these processed aluminum-based metal matrix composites, it contains maximum wear resistance, lesser thermal expansion, and greater withstand of vibrating capability. The aluminum metal matrix compounds like to the top quality appearance even in the poor-based aluminum composites. These materials are come from bielement materials as well

as to be matrix- and ceramic-based material or raw composites in the reinforcing elements [1–3].

In order to get the best material properties when combined with metal matrix composites, the various metals are grouped with the highest reinforced content. The irregular strengthened MMCs or aluminum metal matrix composites (AMMCs) possess lesser hardness and poorer wear resistances are the major factors that would not be reached the maximum attained performances in the tribological characteristics. In their low MMCs or AMMCs, it definitely enhances the mechanical properties when combine to the proper reinforcing particle especially in the nano-based

reinforcing particles and also selecting the process parameters or the processing technique. For that reason, these AMMCs are started in the widespread with aerospace, vehicle, and shipbuilding applications to boost their residential properties top quality in the metal matrix compounds than the unreinforced base material [4–6].

AMMCs disclose updated characteristics in the list below problems like wear resistance, specific mass ratio, abrasion, and rust resistance. Besides, additional buildup is utilized to improve the properties that are attained in the MMCs. For example, damping, electrical as well as thermal conductivity buildings in the textile-based applications as well as it plays a crucial role in the renovation of tribological performances in the numerous usages. From the current research studies, the metal matrix composites had optimum mechanical strength when it is reinforced with nanosized strengthening particles. When MMCs-based composites were being made, low ductility was substituted for good ductility, and this was enhanced simultaneously [7–9].

Additionally, nanosized reinforcements likewise enhance the effectiveness of the metal products as well as ductility structure. Among the various casting processes, the stir casting was the less expensive process and also enhances the mechanical properties from the processed aluminum metal matrix composites. Aluminum-based metal matrix composites generally strengthened by the various nanoceramic particles like silicon carbide, aluminum oxide, titanium oxide, tungsten carbide, and graphene- and boron-based carbides. These reinforcing materials are easily diffused into the any base aluminum alloys. Similarly, the agrowaste product was also prepared as the nanomaterials to produce the metal matrix composites. Some issues are happened during the casting between the base aluminum alloy and other agro-nanoparticles [10–13].

From the various nanoreinforcement particles, nano boron carbide particles are the most hardest particles, maximum stiffness, lesser compressibility, and also provide the better ballistic performance when utilizing with the appropriate aluminum alloys. Consequently, the reduced expense technique from various stir casting processes generated the metal matrix composites and also vortex was executed to develop the mixing in the uniform scattering by use of automated mechanical stirrer.

In this stir casting process, the main issues were wettability and also the melt. It is more called for to get over these concerns with blending of nanostrengthened fragments. Because of the better wettability of nanoparticles, uniform diffusion was generated in the matrix composites. The migration of load was easily moved from the matrix to the strengthened reinforcement in the matrix composite materials. Because of the better bonding structure, it was accumulated while doing so metal matrix composites. It leads to improving the upgraded system to achieve the exceptional mechanical-based characteristics in the nano-processed metal matrix composites [14–19].

From the above detailed reviews, it has been initiated that their metal matrix composites are enhancing the mechanical characteristics and improving the tribological performances. So, this research mainly aims to produce the aluminum-based metal matrix composites from the base material of

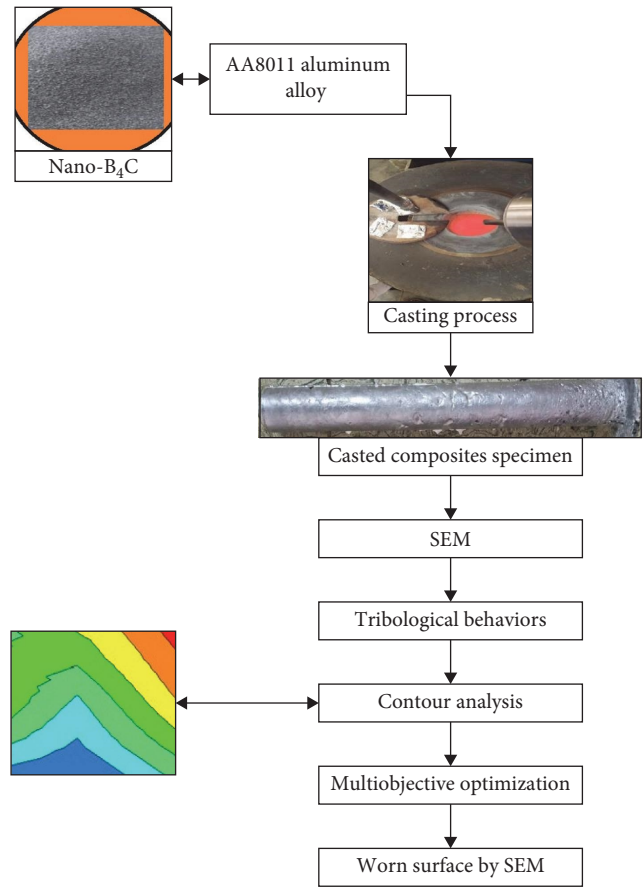


FIGURE 1: Experimental layout.

AA8011 and superior characteristics of nano boron carbide particles and this alloy mainly utilized in the building materials, electrical sectors, and packaging of drugs and food. From the processed nanocomposites, tribological performances were accomplished by the appropriate processing conditions. Then, the tribological behaviors are analyzed by Taguchi-based technique to find the optimal processing parameters. Scanning electron microscope (SEM) analysis was used to measure the wear tracks and confirmation for the presence of nanoparticles during the stir casting process. Figure 1 shows the outline of the graphical abstract.

## 2. Base Material, Nanoparticle Reinforcements, and Preparation of Nano-Based Composites

The predominant aluminum alloy AA8011 was the working material. Due to this, alloy was extremely not hard and right material for space shuttle applications, best heat exchanger component, maximum deep drawing qualities, and other tanking purposes. It contains better features like workability, density, formability, ductility, corrosion resistance, and enhanced mechanical tensile strength. The chemical compositions of AA8011 aluminum alloy are 0.52 of Si, 0.28 of Mg, 0.13 of Cu, 0.028 of Cr, 0.74 of Fe, 0.46 of Mn, 0.084 of Zn, 0.016 of Ti, and balance of aluminum, respectively. In the combinational elements, this aluminum alloy AA8011 was specifically enhances in the aerospace component fabrication. Also, this material

TABLE 1: Tribological process parameters with Taguchi L9.

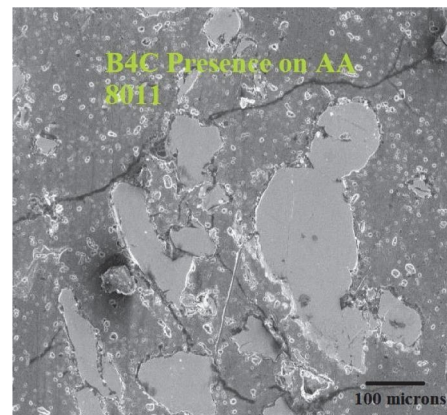
Wear samples order	Sliding velocity (m/s)	Setting wear temperature (°C)	Applied load (N)
1	2.25	30	25
2	2.25	40	35
3	2.25	50	45
4	3	30	35
5	3	40	45
6	3	50	25
7	3.75	30	45
8	3.75	40	25
9	3.75	50	35

was highly used in the maximum-related strength applications and weldments. Based on above situations, this research focused to select the AA8011 aluminum alloy that was the base material. The mechanical properties of AA8011 are 2,689 kg/m<sup>3</sup> of density, 110 MPa of tensile strength, 665°C of melting point, 65 of hardness, and 238 W/mk of thermal conductivity, respectively [20].

Based on the application, the respected base material chosen was the primary factors for every process. But, in this lightweight applications, lightweight metal AA8011 was the selected base material in this investigation. So, this selected base material was utilized as the matrix materials to compose the metal matrix composites with selected appropriate reinforcements. Therefore, in this investigation, proper reinforcements have special features that contain temperature resistance, stiffness, and strength. The processing technique was also important prospects to compose the better metal matrix composites. The specially made lightweight metal matrix composites were prepared by the quicker and easier process. In this way, stir casting process was most reasonable less expensive process over the other solidification techniques. Finally, the completed metastatic arrangements were made on the processed MMCs by the stir casting process. Considering the above issues, in this study, boron carbide with nanosized particles having the 25  $\mu\text{m}$  sizes was selected as the reinforcement material.

Compared to other hardness material like boron nitride and diamond, boron carbide was superior hardened base abrasive material. This boron carbide generally contains superior abrasive characteristics, fabricating components in their specialized materials with less cost than the other reinforcements like aluminum oxide and silicon carbide. The boron carbide materials were highly utilized in the various applications like rocket propellants, welding applications, and defense-based components. The boron carbide also possesses lower thermal conductivity that results in lesser thermal resistance.

Processing technique is also an important factor to produce the aluminum metal matrix composites by the proper features. Therefore, in this investigation, liquid metallurgy-based stir casting process was utilized to compose AMMCs by the influence of aluminum alloy AA8011 and boron carbide nanoparticles. The B<sub>4</sub>C with 15 wt% was mixed with the base alloy of AA8011, which was mixed together by the stir

FIGURE 2: SEM micrographs for stir-casted composites B<sub>4</sub>C/AA8011.

casting process with maintained process parameters like 800°C which was under the guidance of graphite crucible. Before adding of boron carbide into the aluminum alloy under the stir casting, reinforcement particles must be pre-heated at 300°C to eradicate the foreign particles than that the reinforcements were utilized to mixing together in the semi-liquid of AA8011 with proper maintaining parameters at 300 rpm of mechanical stirrer for 5–10 min and stirring speed at 100 m/s. Finally, the molten composites were poured into the mold to ready for the mechanical tests. Then, the solidified composites were attained in the mold which made up of cast iron to compose the cylindrical-based specimens. Next to mold, the required dimension of wear samples having the sizes of 10 and 30 mm of diameter and pin length was achieved to produce the wear performances. As per the condition of G-99, all the specimens were prepared. During the tribological experiments, sliding velocity, setting wear temperature, and applied load were the process parameters to conduct the investigations. The Taguchi L9 method was suitable to design the process parameters for tribological performances and is shown in Table 1. Figure 2 shows the SEM image of processed nanocomposites between B<sub>4</sub>C/AA8011.

As shown in Figure 2, the SEM reveals the presence of boron carbide nanoparticles on the AA8011 by the stir casting process with higher magnification. This image was clearly indicated the presence of boron carbide with homogeneous dispersion within the aluminum alloy AA8011. By adding the 15 wt%, B<sub>4</sub>C was successfully accompanied into

TABLE 2: Wear rate and coefficient of friction on AA8011 and B<sub>4</sub>C nanocomposites.

Wear samples order	Sliding velocity (m/s)	Setting wear temperature (°C)	Applied load (N)	Wear rate (mm <sup>3</sup> /min)	Friction coefficient
1	2.25	30	25	2.451	0.159
2	2.25	40	35	3.684	0.651
3	2.25	50	45	2.985	0.416
4	3	30	35	2.485	0.162
5	3	40	45	3.124	0.528
6	3	50	25	3.951	0.591
7	3.75	30	45	3.012	0.492
8	3.75	40	25	4.005	0.752
9	3.75	50	35	4.415	0.786

the aluminum alloy with appropriated stir casting processing parameters. At the same time, the B<sub>4</sub>C was well synthesized and better dispersion was attained by the liquefying process. Due to the maximum amount of boron carbide, it created the well-bonded structures against the aluminum alloy. The grain boundaries are also well presented and compose the better nanocomposites. Owing to improve the grain boundaries, it reduces the grain structure and the intermetallic particles are well bind together with well-suited optimal processing conditions.

### 3. Results and Discussion

**3.1. Wear Rate and Friction Coefficient on Processed Nano-B<sub>4</sub>C Composites.** The pin on disk tribometer equipment was used to conduct the tribological behavior as per the ASTM of G-99. The working processing conditions of tribological performances were implemented by the following parameters like sliding velocity (2.25–3.75 m/s), setting wear temperature (30–50°C), and applied load (25–45 N), respectively.

The tribometer contains EN-32 that is made of spinning disk having the maximum hardness of 65 HRC which act as the counterweight against the testing sample pin by the influence of the abovementioned processing conditions. Other than the varying process, parameters sliding velocity, setting wear temperature, and applied load, sliding distance was constant for all the level of various process parameters. Before conducting the wear behavior, all the samples were polished as per the standards to improve the surface enhancement on the processed composites. The composites wear specimens were employed to produce the wear rate and coefficient of friction, respectively. As shown in Table 1, all the processing parameters were subjected to conduct the wear test for analyzing the tribological characteristics like wear rate and coefficient of friction. Table 2 shows the outcomes of wear rate and coefficient of friction.

**3.2. Contour Interactions on the Various Tribological Process Parameters on Responses.** Figure 3(a)–3(c) shows the contour experimentation between the various tribological process parameters within the effect of wear rate. Figure 3(a) shows the sliding velocity and wear temperature on the outcomes of wear rate, and it is revealed that the minimum

wear rate was attained between the increasing of sliding velocity from 2.5 to 3.0 m/s and the combinations of wear temperature at less range of 30°C. The lesser wear rate was composed by the presence of boron carbide particles and it was against the sliding and temperature so that the wear rate also enhanced. Figure 3(b) shows the wear temperature and applied load on the processed composites to compose the wear rate, and it is understood that the enhanced wear resistance was highly attained between the combinations of lesser wear temperature and increasing applied load at 25–35 N. Figure 3(c) exhibits the wear performing process parameters like applied load and sliding velocity on the wear rate of the processed nanocomposites of AA8011 and B<sub>4</sub>C, respectively, and it is implicit that the lesser wear was occurred between the lesser sliding velocity and medium of the applied load.

Figure 4(a)–4(c) exhibits the contour investigations involving the assorted tribological process parameters within the consequence of friction coefficient. Figure 4(a) shows the sliding velocity and wear temperature on the upshot of friction coefficient, and it is discovered that the minimum friction was generated between increasing of sliding velocity from 2.5 to 3.0 m/s and the combinations of wear temperature at less range of 30°C. The lesser friction was formed by the existence of maximum weight percentage of boron carbide particles and it was against the sliding and temperature that result in decreasing the friction. Figure 4(b) displays the wear temperature and applied load on the synthesized composites to produce the friction coefficient.

As shown in Figure 4(b), it is implicit that the superior friction coefficient was exceedingly accomplished between the arrangements of slighter wear temperature and rising applied load from 25 to 35 N. Figure 4(c) demonstrates the tribological performing process parameters like applied load and sliding velocity on the friction coefficient of the stir-casted nanocomposites of AA8011 and B<sub>4</sub>C, respectively, and it is implied that the minor friction coefficient was take place between the lower and medium range of sliding velocity (2.25 and 3.0 m/s) and applied load (25 and 35 N). Figure 5 shows the individual responses of wear rate and friction coefficient by the nine various processing conditions.



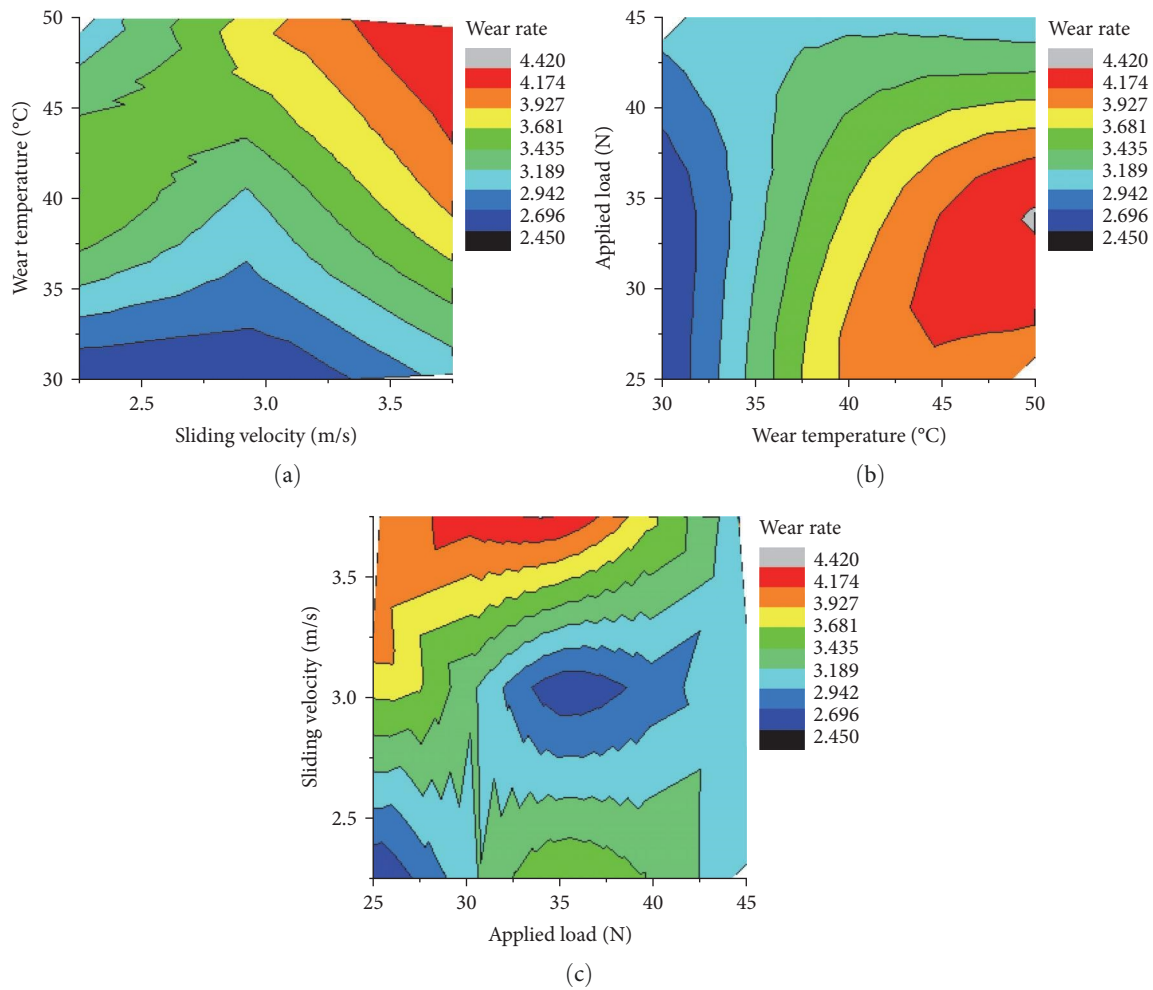


FIGURE 3: (a–c) Tribological process parameters on wear rate.

**3.3. Multiobjective Optimization on the Tribological Responses by Gray Analysis.** In this research, the wear rate and friction coefficient were successfully accomplished by the tribometer technique by the various influencing process parameters like sliding velocity, wear temperature, and applied load. Now those processing parameters required one appropriate technique to validate optimal parameters. Therefore, based on above mentioned issues are resolved by the gray relational analysis [21]. Among the various multiobjective techniques, gray relational analysis was most suited method to solve the difficult issues among the different implemented parameters for any processing. Now, this technique was utilized to confirm that the multiphase parameters were converted into the single objective. In this method, various steps like standardization, calculating the sequence, gray coefficient, and composite gray relational grade (GRG) and ranking method were utilized to produce the optimal process parameters. Table 3 shows the initialization of GRG with outcomes of wear rate and friction coefficient. As shown in Table 3, smaller the better option was implemented to discover the individual sequence of both the responses along with GRG. As shown in Table 3, 0 values were attained at the specimen of 1 and it was further established into the coefficient with gray to find

the composite GRG and best ranking position. Table 4 shows the rank order and its coefficient of wear rate and friction coefficient responses. As shown in Table 4, better composites GRG and best rank were accumulated at the process parameters 2.25 m/s of sliding velocity, 30°C of setting temperature, and 25 N of applied load that compose the better wear rates and lesser friction. Also, the presence of boron carbide reduced the friction between the composite workpiece and counter disk of steel. Figure 6 exhibits the rank arrangements for mixed responses of wear rates and friction coefficient, and sample 1 accommodates rank 1.

**3.4. Worn Surface Analysis of Processed Nano Boron Carbide and AA8011 Composites.** Figures 7 and 8 show the micrograph of worn surface on the processed nanocomposites between the AA8011 and boron carbide, and belong to the worn surfaces of optimal parameters at 2.25 m/s of sliding velocity, 30°C of wear temperature and 25 N of applied load and poor parameters at 3.75 m/s of sliding velocity, 50°C of wear temperature, and 35 N of applied load, respectively. As shown in Figure 7, SEM analysis reveals that the wear track was slightly formed due to the maximum content of B<sub>4</sub>C that was occupied to resist the wear which results in less wear

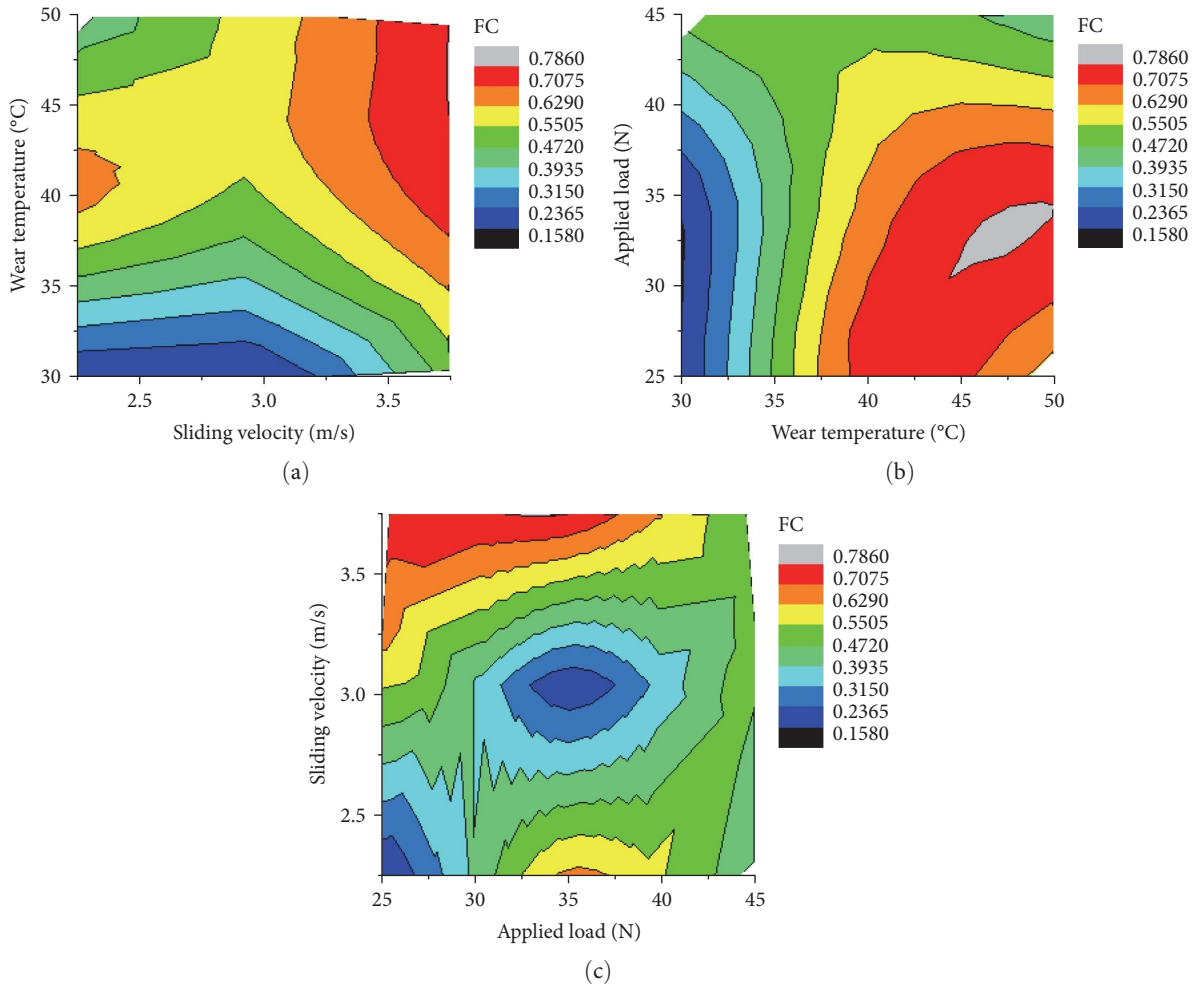


FIGURE 4: (a–c) Tribological process parameters on friction coefficient.

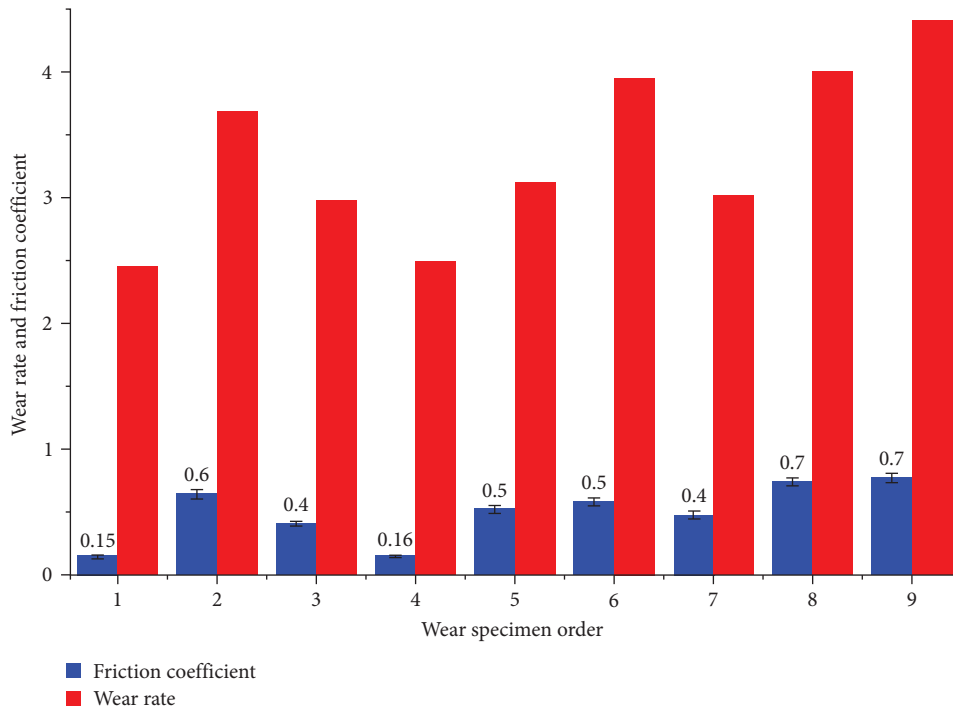


FIGURE 5: Wear rate and friction coefficient on various wear specimens.

TABLE 3: Standardization and sequence of GRG on processed composites.

Wear samples order	Wear rate (mm <sup>3</sup> /min)	Friction coefficient	Standard GRG (WR)	Standard GRG (FC)	Sequence GRG (WR)	Sequence GRG (FC)
1	2.451	0.159	0.000	0.000	0.000	0.000
2	3.684	0.651	-0.628	-0.785	0.628	0.785
3	2.985	0.416	-0.272	-0.410	0.272	0.410
4	2.485	0.162	-0.017	-0.005	0.017	0.005
5	3.124	0.528	-0.343	-0.589	0.343	0.589
6	3.951	0.591	-0.764	-0.689	0.764	0.689
7	3.012	0.492	-0.286	-0.531	0.286	0.531
8	4.005	0.752	-0.791	-0.946	0.791	0.946
9	4.415	0.786	-1.000	-1.000	1.000	1.000

GRG, gray relational grade.

TABLE 4: Gray coefficient and rank position of wear rates and friction coefficient.

Wear samples order	Wear rate (mm <sup>3</sup> /min)	Friction coefficient	Coefficient (WR)	Coefficient (FC)	Mixed GRG	GRG rank
1	2.451	0.159	1.000	1.000	1.000	1
2	3.684	0.651	0.443	0.389	0.416	6
3	2.985	0.416	0.648	0.550	0.599	3
4	2.485	0.162	0.967	0.991	0.979	2
5	3.124	0.528	0.593	0.459	0.526	5
6	3.951	0.591	0.396	0.421	0.408	7
7	3.012	0.492	0.636	0.485	0.561	4
8	4.005	0.752	0.387	0.346	0.367	8
9	4.415	0.786	0.333	0.333	0.333	9

GRG, gray relational grade.

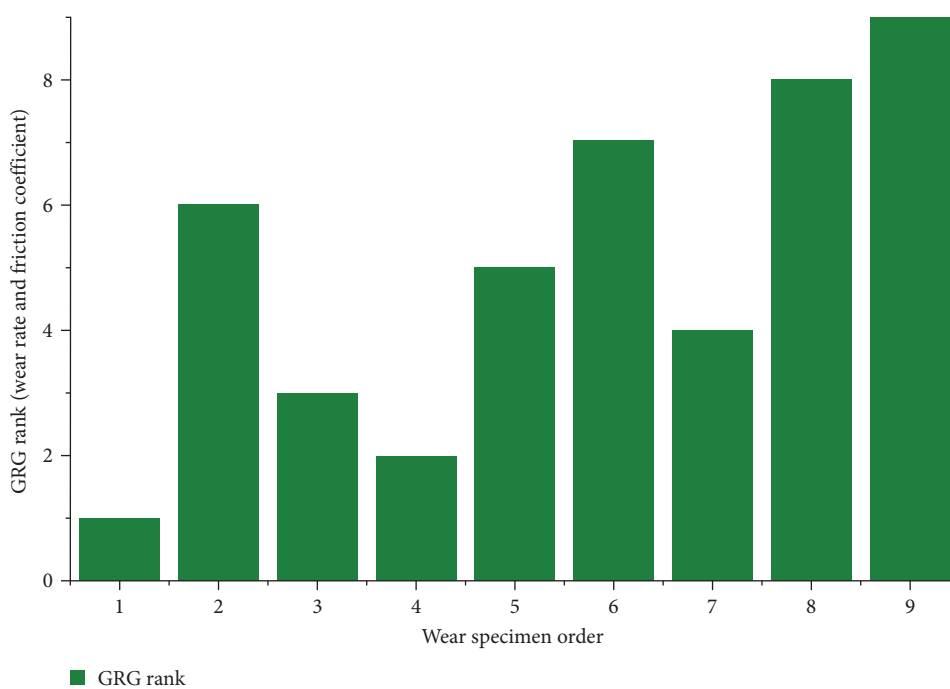


FIGURE 6: Gray relational grade rank for wear rates and friction coefficient.

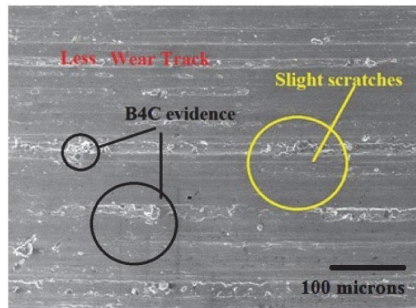


FIGURE 7: SEM worn surfaces on optimal parameters.

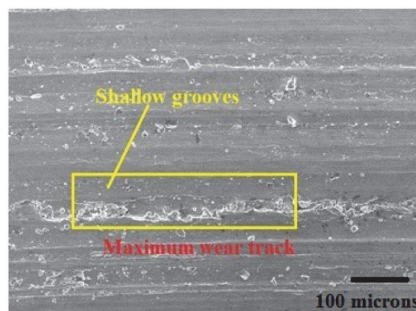


FIGURE 8: SEM worn surfaces on poorer parameters.

track that was formed. Process parameters were major reason to reduce the wear track due to less wear temperature along with less sliding velocity and low applied load. As shown in Figure 8, it was understood that the SEM analysis presents the maximum wear track that was generated by the maximum of sliding velocity and applied load. By utilizing maximum temperature, setting was initiated to improve the wear rate and coefficient of friction. At the same time, both processed composite specimens produced the better results due to the presence of boron carbide and this particles resist the sliding distance and maximum working load. The maximum weight percentage (15 wt%) was the major reason to enhance the better wear resistance and lesser coefficient of friction. It is revealed that the maximum frictional heat was generated between the specimen and counter disk, so that the heat was not increased on the specified composites by the presence of nano boron carbide particles [20–25]. The presence of nanosized boron carbide was a major aspect to improve their wear rates and similarly, the lesser setting temperature was another reason to reduce the wear tracks.

#### 4. Conclusion

In this research, aluminum alloy AA8011 and nano boron carbide particles were successfully synthesized by the liquefy stir casting process. During the casting process, appropriate setting conditions like mechanical stirrer speed, melting temperature, and preheating temperatures were accurately utilized to compose the better nanocomposites. The tribological behaviors like sliding velocity, setting wear temperature, and applied load were majorly influence to compose the fine wear rates and lesser friction coefficient during the process of

nanocomposites. The multiobjective optimization technique of gray method effectively produced the optimal process parameters from the L9 Taguchi design. The maximum wear resistance and minimum coefficient of friction were composed at the parameters at 2.25 m/s of sliding velocity, 30°C of wear temperature, and 35 N of working load. Similarly, the SEM micrograph reveals that the presence of boron carbide on the AA8011 aluminum alloy showed the fine particles by the uniform arrangements during the stir casting process.

#### Data Availability

The data used to support the findings of this study are included within the article.

#### Conflicts of Interest

The authors declare that they have no conflicts of interest.

#### References

- [1] A. E. A. Al-maamari, A. K. M. A. Iqbal, and D. M. Nuruzzaman, "Mechanical and tribological characterization of self-lubricating Mg–SiC–Gr hybrid metal matrix composite (MMC) fabricated via mechanical alloying," *Journal of Science: Advanced Materials and Devices*, vol. 5, no. 4, pp. 535–544, 2020.
- [2] D. Bartkowski and G. Kinal, "Microstructure and wear resistance of Stellite-6/WC MMC coatings produced by laser cladding using Yb:YAG disk laser," *International Journal of Refractory Metals and Hard Materials*, vol. 58, pp. 157–164, 2016.
- [3] O. B. Bembalge and S. K. Panigrahi, "Exploring a hybrid manufacturing process to develop high performance age hardenable ultrafine grained AA6063/SiC nano-composite sheets," *Journal of Manufacturing Processes*, vol. 70, pp. 508–517, 2021.
- [4] S. Devaraj, R. Malkapuram, and B. Singaravel, "Performance analysis of micro textured cutting insert design parameters on machining of Al-MMC in turning process," *International Journal of Lightweight Materials and Manufacture*, vol. 4, no. 2, pp. 210–217, 2021.
- [5] A. M. El-khatib, I. I. Bondouk, K. M. Omar, A. Hamdy, and M. El-khatib, "Impact of changing electrodes dimensions and different ACs on the characteristics of nano composites NZnO/MWCNTs prepared by the arc discharge method," *Surfaces and Interfaces*, vol. 29, Article ID 101736, 2022.
- [6] V. Khalili, C. Sengstock, Y. Kalchev, J. Pftzing-Micklisch, and J. Frenzel, "Exploring MgO/HA ceramic nano-composites for biodegradable implants: exploring biological properties and micromechanics," *Surface and Coatings Technology*, vol. 445, Article ID 128730, 2022.
- [7] S. Khoshshima, S. Mertdinç, A. Motallebzadeh, Z. Altıntaş, D. Ağaoğulları, and Ö. Balcı-Çağırın, "Enhanced hardness and wear resistance of Al-based hybrid MMCs by using of composite metal boride reinforcement particles," *Materials Chemistry and Physics*, vol. 288, Article ID 126377, 2022.
- [8] L. Tharanikumar, B. Mohan, and G. Anbuhezhiyan, "Enhancing the microstructure and mechanical properties of Si<sub>3</sub>N<sub>4</sub>–BN strengthened Al–Zn–Mg alloy hybrid nano composites using vacuum assisted stir casting method," *Journal of Materials Research and Technology*, vol. 20, pp. 3646–3655, 2022.



- [9] U. Müller, S. Prinz, S. Barth, and T. Bergs, "Simulation of friction between diamond and polycrystalline cubic boron nitride," *Procedia CIRP*, vol. 104, pp. 44–49, 2021.
- [10] A. Naeimi, F. E. Ghadi, S. M. Saadatkhah, and M. Honarmand, "First and efficient bio-nano composite, SnO<sub>2</sub>/Calcite based on Cypress leaves and eggshell wastes, for cytotoxic effects on HepG2 liver cancer cell lines and its antioxidant and antimicrobial activity," *Journal of Molecular Structure*, vol. 1259, Article ID 132690, 2022.
- [11] K. Ramasubramanian, N. Arunachalam, and M. S. Ramachandra Rao, "Wear performance of nano-engineered boron doped graded layer CVD diamond coated cutting tool for machining of Al-SiC MMC," *Wear*, vol. 426–427, Part B, pp. 1536–1547, 2019.
- [12] H. Shi, Z. Dou, Y. Meng, and T. Zhang, "Effects of reactants proportions on features of in-situ magnesiothermic self-propagating high temperature synthesized boron carbide powder," *Ceramics International*, vol. 48, no. 22, pp. 33400–33411, 2022.
- [13] S. Sankara Raju, G. Srinivasa Rao, and C. Samantra, "Wear behavioral assessment of Al-CSAp-MMCs using grey-fuzzy approach," *Measurement*, vol. 140, pp. 254–268, 2019.
- [14] J. C. Songara, J. N. Patel, and A. A. Mungray, "Preparation and characterization of PAA/GG-zeolite nano-composite hydrogel for agricultural applications," *Journal of the Indian Chemical Society*, vol. 99, no. 10, Article ID 100686, 2022.
- [15] S. Thangaraj, G. M. Pradeep, M. S. Heaven Dani, S. Mayakannan, and A. Benham, "Experimental investigations on tensile and compressive properties of nano alumina and arecanut shell powder reinforced polypropylene hybrid composites," *Materials Today: Proceedings*, vol. 68, Part 6, pp. 2243–2248, 2022.
- [16] T. Wang, X. Liu, S. Chen, J. Lei, and X. Song, "Study on microstructure and tribological properties of nano/micron TiC/TC4 composites fabricated by laser melting deposition," *Journal of Manufacturing Processes*, vol. 82, pp. 296–305, 2022.
- [17] Y. Wang, Y.-D. Wu, and G.-H. Zhang, "Boronation reaction between molybdenum or tungsten powder and boron carbide in aluminium melt," *International Journal of Refractory Metals and Hard Materials*, vol. 105, Article ID 105813, 2022.
- [18] H. Werheit, B. Herstell, W. Winkelbauer et al., "Electrical conductivity of boron carbide from ~5 to ~2100 K in the whole homogeneity range," *Solid State Sciences*, vol. 132, Article ID 106987, 2022.
- [19] V. Zamora, F. J. Martínez-Vázquez, F. Guiberteau, and A. L. Ortiz, "Spark-plasma sintering of boron carbide–silicon carbide composites at 1400°C from B<sub>4</sub>C + Si: densification and sintering/reaction mechanisms," *Journal of the European Ceramic Society*, vol. 42, no. 15, pp. 6876–6888, 2022.
- [20] A. Aabid, M. A. Murtuza, S. A. Khan, and M. Baig, "Optimization of dry sliding wear behavior of aluminium-based hybrid MMC's using experimental and DOE methods," *Journal of Materials Research and Technology*, vol. 16, pp. 743–763, 2022.
- [21] C. Chanakyan, S. Sivasankar, M. Meignanamoorthy, and S. V. Alagarsamy, "Parametric optimization of mechanical properties via FSW on AA5052 using Taguchi based grey relational analysis," *Incas Bulletin*, vol. 13, no. 2, pp. 21–30, 2021.
- [22] W. Zhang, "A novel ceramic with low friction and wear toward tribological applications: boron carbide–silicon carbide," *Advances in Colloid and Interface Science*, vol. 301, Article ID 102604, 2022.
- [23] F. Xiao, M.-X. Wu, Y.-X. Wang et al., "Effect of trace boron on grain refinement of commercially pure aluminum by Al–5Ti–1B," *Transactions of Nonferrous Metals Society of China*, vol. 32, no. 4, pp. 1061–1069, 2022.
- [24] A. Sharma, S. Dixit, N. Baler, P. Agrawal, S. K. Makineni, and K. Chattopadhyay, "Impact of boron as an alloying addition on the microstructure, thermo-physical properties and creep resistance of a tungsten-free Co-base  $\gamma/\gamma'$  superalloy," *Materials Science and Engineering: A*, vol. 855, Article ID 143899, 2022.
- [25] S. Bakkar, S. Thapliyal, N. Ku et al., "Controlling anisotropy of porous B<sub>4</sub>C structures through magnetic field-assisted freeze-casting," *Ceramics International*, vol. 48, no. 5, pp. 6750–6757, 2022.